

Observation of transition from escape dynamics to underdamped phase diffusion in a Josephson junction

J.M. Kivioja,¹ T.E. Nieminen,¹ J. Claudon,² O. Buisson,² F.W.J. Hekking,³ and J.P. Pekola¹

¹*Low Temperature Laboratory, Helsinki University of Technology, POB 3500, FIN-02015 HUT, Finland*

²*Centre de Recherches sur les Très Basses Températures, laboratoire associé à l'Université Joseph Fourier, C.N.R.S., BP 166, 38042 Grenoble-cedex 9, France*

³*Laboratoire de Physique et Modélisation des Milieux Condensés,*

C.N.R.S. and Université Joseph Fourier, B.P. 166, 38042 Grenoble Cedex 9, France

(Dated: April 4, 2005)

We have investigated the dynamics of underdamped Josephson junctions with relatively small Josephson coupling E_J . In addition to the usual crossover between macroscopic quantum tunnelling and thermally activated (TA) behavior we observe, for the first time, the transition from TA behavior to underdamped phase diffusion. Above the crossover temperature the threshold for switching into the finite voltage state becomes extremely sharp. We propose a (T, E_J) phase-diagram with various regimes and show that for a proper description of its dissipation and level quantization in a metastable well are crucial.

PACS numbers: 74.50.+r, 85.35.-p, 85.25.Dg

Keywords: Josephson junction, phase diffusion, energy level quantization

A hysteretic Josephson junction (JJ) switching from its metastable zero-voltage state into a stable finite voltage state has recently been used as a read-out device for superconducting quantum bit systems in many experiments [1]. Switching measurements also enable one to perform conventional large bandwidth current measurements, and recently there have been proposals to use hysteretic JJs as ammeters for studying phenomena like non-Gaussian noise [2]. Often it may be advantageous to reduce the critical current I_c of the detecting junction in order to increase the measurement sensitivity. Yet the physics governing switching phenomena of small I_c junctions ultimately differs from those with larger I_c [3]. How far can one reduce I_c still maintaining the useful features of the detector? Despite a considerable amount of work on junctions with moderate I_c [4], no clear picture based on a systematic study exists as yet of temperature-dependent escape phenomena in such junctions. In this Letter we present such a study.

The dynamical variable of a JJ is the phase difference φ of the superconducting wavefunction in the two electrodes. Within the RCSJ (Resistively and Capacitively Shunted Junction) model, the dynamics of φ is governed by the Josephson energy $E_J = \hbar I_c / 2e$, the charging energy $E_C = e^2 / 2C_J$ (C_J is the junction capacitance), and a shunt resistance R responsible for dissipation. For later use we also define the bare plasma frequency $\omega_p = \sqrt{8E_J E_C} / \hbar$ and the quality factor $Q = \omega_p R C$. As we will detail below, the behavior of the junction at a given temperature T can be classified according to the phase diagram of Fig. 1a. The overdamped case $Q < 1$ with $E_J \gtrsim E_C$ was studied in detail by Vion *et al.* [3], who uncovered the existence of a phase diffusion regime at finite T with the appearance of a small voltage, prior to switching to a voltage of the order of twice the su-

perconducting gap Δ [5]. As far as the underdamped case $Q > 1$ is concerned, most experiments were done on junctions with relatively high I_c . Depending on T such junctions escape out of the metastable zero-voltage state either via macroscopic quantum tunnelling (MQT) or thermal activation (TA) processes, switching directly to the finite-voltage state. In this Letter we focus on the regime $Q > 1$ with relatively small I_c , such that $E_J \sim k_B T \gg E_C$. We show, theoretically and experimentally, that a regime exists where escape does not lead to a finite voltage state but rather to underdamped phase diffusion (UPD, the shaded region in Fig. 1a).

According to the RCSJ model, the dynamics of a JJ biased with a current I is that of a particle (mass $m = \hbar^2 / 8E_C$) whose position is φ . It moves in a tilted cosine potential $U(\varphi) = -E_J [\cos\varphi + (I/I_c)\varphi]$ under a viscous force $(\frac{\hbar}{2e})^2 \frac{d\varphi}{Rdt}$. The bias current renormalizes the plasma frequency, such that $\omega_p = \sqrt{d^2 U / md\varphi^2} = \sqrt{8E_J E_C q_0} / \hbar$ with $q_0 = \sqrt{2(1 - I/I_c)}$. The cosine potential has wells where the particle can be localized; φ then has constant average value, and the average voltage across the junction is zero. For non-zero I the quantum levels in the potential well are metastable and the particle can escape from a given well either via TA over, or MQT through the barrier. For large junctions $\Gamma_{TA}(I, T) = \frac{\omega_p}{2\pi} e^{-\frac{\Delta U}{k_B T}}$ for the TA escape rate and $\Gamma_{MQT}(I) = 12\sqrt{6\pi} \frac{\omega_p}{2\pi} \sqrt{\Delta U / \hbar \omega_p} e^{-\frac{36}{5} \frac{\Delta U}{\hbar \omega_p}}$ for the MQT rate [6]. In the cubic approximation the barrier height is $\Delta U = \frac{2}{3} E_J q_0^3$. Below the cross-over temperature $T_0 = \hbar \omega_p / 2\pi k_B$ the dominant escape mechanism is MQT. Approximating the total escape rate as $\Gamma_\Sigma(I, T) \simeq \Gamma_{TA}(I, T) + \Gamma_{MQT}(I)$, the escape probability in the time interval $0 \leq t \leq \tau$ can be written as $P_\Sigma(I, T) = 1 - e^{-\int_0^\tau \Gamma_\Sigma(I, T) dt}$. If dissipation is weak,

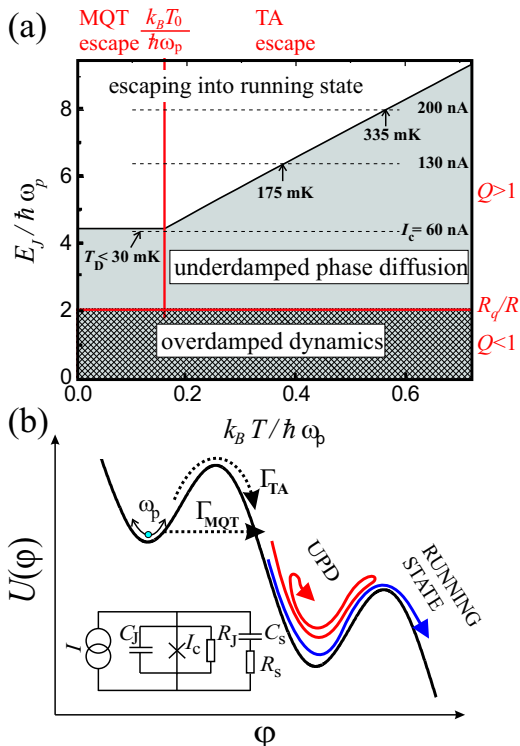


FIG. 1: (a) The various operation regimes of a Josephson junction with low E_J . For details, see text. The UPD regime corresponds to $R_s = 500 \Omega$, $C_J = 100$ fF and $\tau = 100 \mu\text{s}$. (b) The dynamics in the upper well and schematic behavior upon escape. Inset: equivalent circuit of the junction with frequency dependent dissipation.

upon escape from the well the particle moves down the potential and phase is running freely, hence the voltage reaches a finite value, about 2Δ . However, if dissipation is strong enough, there is a finite probability that, upon escape from the well, the particle is relocalized in the next well instead of running down the potential: the phase then diffusively moves from one metastable well to another, see Fig. 1b. In this UPD regime the average voltage across the junction is much smaller than 2Δ [3].

As it was pointed out over a decade ago [7], phase diffusion can occur even in a hysteretic junction due to the dependence of dissipation on frequency ω [4]. Our experiment corresponds to the simplified equivalent circuit with frequency dependent dissipation as presented in the inset of Fig. 1(b). After switching to the running state, the dominant part of dissipation comes from small ω , governed by $R(\omega \sim 0)$, typically given by the large junction subgap resistance, of the order of $1 \text{ M}\Omega$. In the phase diffusion regime the phase mainly oscillates in a well at the plasma frequency and thus the dissipation is characterized by $R(\omega_p)$, which is much smaller, typically of the order of vacuum impedance $Z_0 \approx 377 \Omega$, since C_s

(Fig. 1b) acts as a short. Here we will consider junctions that are underdamped even at ω_p , in contrast to [3].

The dissipated energy between neighboring potential maxima can be approximated by $E_D \approx 8E_J/Q$ and if the particle has energy less than E_D above the *next* barrier top, it simply diffuses to the next well. The maximum possible dissipated power due to phase diffusion can be written as $\frac{1}{2\pi} \frac{2eV}{\hbar} E_D$, where V is the average voltage across the junction. By equating this with the applied bias power $I_m V$, we find the maximum possible phase diffusion current $I_m = 4I_c/\pi Q$, which is identical in form to the well known retrapping current formula, but now the value of Q is that at plasma frequency ω_p . For $I < I_m$, there is non-zero probability that phase relocalizes after escape. The grey area in Fig. 1(a) presents the UPD regime, where escape does not necessarily lead to the transition into a running state. The condition $\Gamma_{TA}(I_m, T_D) \approx 1/\tau$ determines the separatrix $E_J^D(T_D)$ between TA and UPD regions in Fig. 1(a) with current pulses of length τ :

$$E_J^D \approx \frac{3}{2} k_B T_D (1 - I_m/I_c)^{-3/2} \ln(\omega_p \tau / 2\pi). \quad (1)$$

Similarly, for $T < T_0$, the separatrix between MQT and UPD is found from $\Gamma_{MQT}(I_m) \approx 1/\tau$; E_J^D is independent of T , and given by Eq. (1) with T_0 replacing T_D .

We present experimental data of two samples, a dc-SQUID and a single JJ. They were fabricated using standard electron beam lithography and aluminum metallization in a UHV evaporator. The AlOx tunnel barriers were formed by basic room temperature oxidation of Al. The dc-SQUID consists of two wide superconducting planes connected by two short superconducting lines with tunnel junctions in the middle forming the dc-SQUID loop of area $20 \times 39 (\mu\text{m})^2$ (see the inset in Fig. 2). The loop inductance was determined [8] to be around 100 pH , small as compared to the calculated Josephson inductance ($L = \frac{\Phi_0}{2\pi I_c} = 400 \text{ pH}$ per junction). The dc-SQUID thus behaves almost like a single JJ, whose I_c can be tuned. The other measured sample was a single junction between long inductive biasing lines. The normal state resistances of the dc-SQUID and the single JJ were $1.3 \text{ k}\Omega$ and $0.41 \text{ k}\Omega$ yielding for I_c 199 nA and 630 nA , respectively. Assuming a specific value of $50 \text{ fF}/(\mu\text{m})^2$, the capacitances of the samples were estimated to be 100 fF and 130 fF , respectively. Both measured samples had strongly hysteretic IV -characteristics with retrapping currents well below 1 nA .

The experimental setup is presented in the inset in Fig. 2. Switching probabilities have been measured by applying a set of trapezoidal current pulses through the sample and by measuring the number of resulting voltage pulses. At the sample stage we used low pass RC -filters (surface mount components near the sample). In the measurements on a single junction we used surface mount capacitors ($C_s = 680 \text{ pF}$), but in the dc-SQUID

measurements we had π -filters in series with resistors, with $C_s \sim 5$ nF capacitance to ground. The resistors were $R_s = 500 \Omega$ and 680Ω in the measurement on a dc-SQUID and on a single junction, respectively. Bonding wires with inductance of order nH connect the sample to filters.

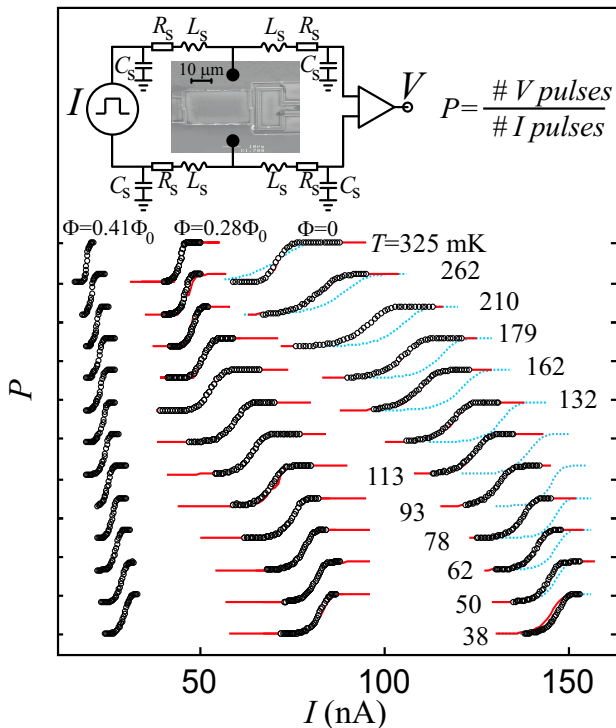


FIG. 2: Cumulative histograms of the dc-SQUID at different temperatures and at different magnetic fields. Curves are shifted for clarity and the vertical spacing between ticks corresponds to unity escape probability. Solid lines are from simulations described in the text; dotted blue lines correspond to $P_\Sigma(I, T)$. Inset: scanning electron micrograph of the measured dc-SQUID and the experimental circuit.

In Fig. 2 we present the measured cumulative switching histograms (open circles) of the dc-SQUID at different fluxes Φ and temperatures with $\tau = 200 \mu\text{s}$. At the lowest temperatures, the histograms can be well fitted by the MQT model, giving $I_c = 200$ nA, 128 nA and 55 nA, for $\Phi/\Phi_0 = 0, 0.28$ and 0.41 respectively. For $\Phi = 0$ we also plot the escape probability $P_\Sigma(I, T)$ defined earlier (dotted blue lines). In Fig. 3 we show the measured histogram position $I_{50\%}$ [$P(I_{50\%}) \equiv 0.5$] and the width ΔI ($\equiv I_{90\%} - I_{10\%}$) for both samples. The dc-SQUID measurements were done both at negative and positive values of flux in order to ensure that the external flux had not changed. The position in Fig. 3(a) is normalized to the corresponding value of I_c at zero temperature. At low T all the measured value data are consistent with MQT results. On increasing T the parameters are constant up to the estimated cross-over temperature T_0 . For $T > T_0$ the width is increasing and the position is moving down

as TA model predicts. The qualitative agreement is good for most of the results up to the temperature T_D . At T_D , ΔI starts to decrease abruptly. Moreover, the position $I_{50\%}$ saturates at the same value $\simeq 0.35I_c$. For the single JJ, the saturation occurs at $\simeq 0.3I_c$. The dc-SQUID data measured at $\Phi = \pm 0.41\Phi_0$ show no trace of thermal activation at any temperature, and underdamped phase diffusion prevails down to temperatures below $T_0 \simeq 50$ mK where MQT dominates.

If we assume a realistic shunt impedance $R(\omega_p) \simeq 500 \Omega$ (the value of the surface mount resistors), we obtain $Q \approx 4$ at $I_c = 200$ nA and $C_J = 100$ fF, which yields $I_m \simeq 0.35I_c$, like in the experiment. In the diagram of Fig. 1 we also present I_c of the dc-SQUID at fluxes 0, $\pm 0.28\Phi_0$ and $\pm 0.41\Phi_0$ by horizontal dashed lines. It can be seen that the intersections of the dashed lines and the boundary of the UPD regime are very close to the experimental values of T_D . The saturation of the histograms and their re-entrant steepness is thus a manifestation of the cross-over from TA escape into UPD due to dissipation. In the case of a single JJ we obtain $I_m \approx 0.3 I_c$ and

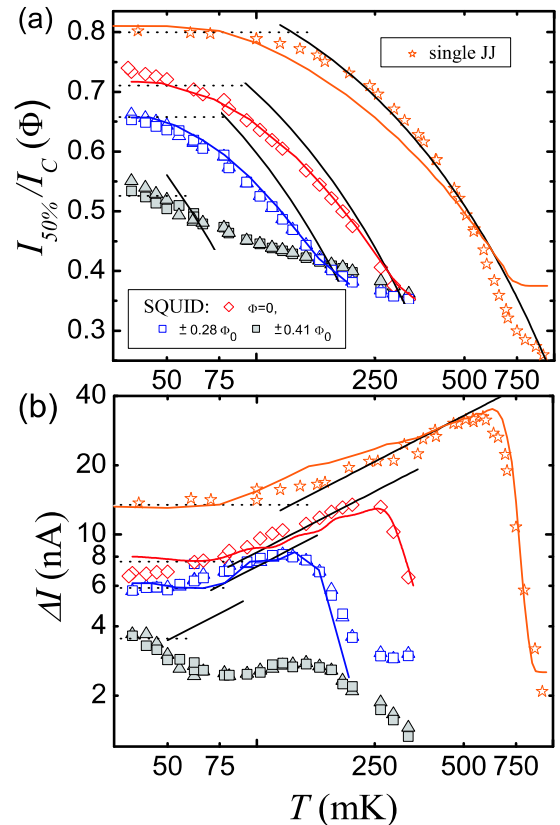


FIG. 3: (a) The positions ($I_{50\%}$) and (b) the widths (ΔI) of the histograms. Black solid and dotted lines are results (with known junction parameters) of standard TA and MQT models, respectively, ignoring dissipation. Blue, red and orange solid lines are the parameters of the simulated histograms based on the LO model discussed in the text.

$T_D \approx 650$ mK, yielding $Q = 4.4$. This corresponds to $R(\omega_p) \simeq 230 \Omega$, somewhat smaller than the anticipated value $R(\omega_p) \simeq 680 \Omega$.

Fig. 2 shows that the standard TA and MQT models cannot account for our observations. Except for the data at the lowest temperatures the measured histograms deviate from $P_\Sigma(I, T)$. Dissipation alone cannot explain the difference. The basic TA model yields a width $\Delta I \propto T^{2/3}$ [6] and it can be seen in Figs. 2 and 3 that the dc-SQUID has weaker temperature dependence even well below T_D . In the dc-SQUID there are just few energy levels in the well and thus the assumptions of continuous energy spectrum are not valid [6]. Within the semiclassical model of Larkin and Ovchinnikov (LO) [9] the total escape probability is calculated using $P_{LO}(\tau) = 1 - \sum_k \rho_k(\tau)$, where $\rho_k(\tau)$ is the probability of finding the particle in a state k after the current pulse of length τ . The kinetic equation can be written as $\frac{d\rho_k}{dt} = \sum_j (\gamma_{jk}\rho_j - \gamma_{kj}\rho_k) - \Gamma_k\rho_k$. We take into account transitions γ_{jk} between neighboring levels and tunnelling out, Γ_k . The relaxation rates between levels j and $j-1$ are well approximated by $\gamma_{j-1,j} = j\omega_p/4Q$. Detailed balance yields $\gamma_{j,j-1} = e^{-\beta(E_j - E_{j-1})}\gamma_{j-1,j}$. The positions of the levels and the escape rates are calculated using the results of Ref. [9]. The final state $\bar{\rho} \equiv [\rho_1 \ \rho_2 \ \dots \ \rho_k]$ is calculated numerically using $\bar{\rho}(\tau) = \frac{1}{\tau} \int_0^\tau e^{\mathbf{A}(t)} \bar{\rho}(0) dt$, where \mathbf{A} is the transition matrix. I is set to zero in the beginning, and $\bar{\rho}(0)$ is Boltzmann distributed.

The effect of the relocating dissipation must be taken into account also in the quantized energy level model. Using again $E_D = 8E_J/Q$, and the fact that the energy difference between the two successive maxima is $-2\pi E_J I/I_c$, the level energy E must satisfy

$$\Delta U - E < E_J (2\pi I/I_c - 8/Q) \quad (2)$$

to allow switching into the free running state. If (2) is violated, the corresponding tunnelling rate is set to zero [10]. Note that (2) yields the condition $I > I_m$ if we set $\Delta U = E$, but in Eq. (2) we assume that after tunnelling the starting point is not at the potential maximum. The solid red lines in Fig. 2 present results of simulations with quantized energy levels and dissipation for the data of the dc-SQUID at zero and $\pm 0.28\Phi_0$ fluxes. At $\pm 0.41\Phi_0$ I_c is so small that the escape probability is large even at zero bias (except at the lowest temperatures). This means that the phase is moving constantly rather than infrequently escaping from a localized state, and thus our model does not work anymore. The only fitting parameter was Q , and the fitted values were in a very reasonable range. At $\Phi = 0$ we find $Q \approx 6$ at the lowest temperature, and it decreases with increasing temperature up to 4 at 325 mK. At $\pm 0.28\Phi_0$ $Q \approx 3$ to 4, again decreasing with temperature. In Fig. 3 we present $I_{50\%}$ and ΔI of the simulated histograms. We present also the simulated parameters for single junction ($Q \approx 4$) [5]. In the measurements on a single junction, the number of energy levels

is large (≈ 20) and their separation is smaller than their width. Our model assumes well-separated levels and thus the agreement with a simple TA model is better for a single junction at $T < T_D$, especially in Fig. 3 (a), whereas re-entrant steepness of the histograms could not be explained with the basic TA model. The agreement between simulation and measurements on a dc-SQUID is excellent. The position and the width of the measured histograms coincide and, in particular, at higher temperatures the simulated histograms for both samples start to get steeper again. At higher temperatures the upper energy levels, whose escape rate is significant with smaller potential tilting angles, are populated as well. The histograms thus peak at smaller currents and the condition (2) is not necessarily fulfilled anymore. What remains in the measured (and simulated) histograms is the escape from the states at the tail of the Boltzmann distribution above the dissipation barrier.

In summary, our measurements demonstrate for the first time how a Josephson junction can transit from the macroscopic quantum tunnelling through thermal activation into underdamped phase diffusion under the variation of temperature and magnetic flux. A model including a phase diffusion barrier and level quantization yields a quantitative fit of the observations.

Note added: since the submission of this manuscript, similar experimental results were reported by Krasnov et al. [11]. Their interpretation differs from ours in details.

The Academy of Finland, EU IST-FET-SQUBIT2 and the French ACI, IPMC and IUF programs are acknowledged for financial support. We thank J. Männik, A. O. Niskanen, T.T. Heikkilä and M.A. Paalanen for helpful discussions.

-
- [1] D. Vion *et al.*, Science **296**, 886 (2002); I. Chiorescu *et al.*, Nature **431**, 159 (2004); S.Saito *et al.*, Phys. Rev. Lett. **93**, 037001 (2004); J. Claudon *et al.*, *ibid.* **93**, 187003 (2004)
 - [2] J. Tobiska and Yu. V. Nazarov, Phys. Rev. Lett. **93**, 106801 (2004); J.P. Pekola, *ibid.* **93**, 206601 (2004).
 - [3] D. Vion *et al.*, Phys. Rev. Lett. **77**, 3435 (1996).
 - [4] A. Franz *et al.*, Phys. Rev. B **69**, 014506 (2004); Y. Koval, M.V. Fistul, and A. V. Ustinov, Phys. Rev. Lett. **93**, 087004 (2004); P.A. Warburton *et al.*, J. Appl. Phys. **95**, 4941 (2004); Joachim Sjöstrand *et al.*, cond-mat/0406510 (2004).
 - [5] In this paper, we ignore the T -dependence of Δ .
 - [6] U. Weiss, *Quantum Dissipative Systems*, (World Scientific, Signapore, 1999), 2nd ed.
 - [7] J.M. Martinis and R.L. Kautz, Phys. Rev. Lett. **63**, 1507 (1989); R.L. Kautz and J.M. Martinis, Phys. Rev. B **42**, 9903 (1990).
 - [8] H.S.J. van der Zant, D. Berman and T.P. Orlando, Phys. Rev. B **49**, 12945 (1994).
 - [9] A. I. Larkin and Yu. N. Ovchinnikov, Zh. Eksp. Teor. Fiz **91**, 318 (1986)[Sov. Phys. JETP **64**, 185 (1987)]; A.

I. Larkin and Yu. N. Ovchinnikov, Zh. Eksp. Teor. Fiz **87**, 1842 (1984) [Sov. Phys. JETP **60**, 1060 (1984)].

[10] With the low Q values in the experiment, the phase relaxes in the next well in a time $\sim \omega_p^{-1} \sim 100$ ps, far

shorter than the typical time interval between phase diffusion events (10...100 μ s for bias currents used here).

[11] V.M. Krasnov *et al.*, cond-mat/0503067.